Nat. Hazards Earth Syst. Sci. Discuss., https://doi.org/10.5194/nhess-2017-273
Manuscript under review for journal Nat. Hazards Earth Syst. Sci.
Discussion started: 31 July 2017

Natural Hazards and Earth System Sciences
Discussions

Satellite-based emergency mapping: Landslides triggered by the 2015 Nepal earthquake

Jack G. Williams, Nick J. Rosser, Mark E. Kincey, Jessica Benjamin, Katie J. Oven, Alexander L. Densmore, David G. Milledge, and Tom R. Robinson

Institute of Hazard, Risk and Resilience and Department of Geography, Durham University, Lower Mountjoy, South Road, Durham. UK. DH1 3LE

Correspondence to: Jack G. Williams (j.g.williams@durham.ac.uk)

Abstract. Landslides triggered by large earthquakes in mountainous regions contribute significantly to overall earthquake losses and pose a major secondary hazard that can persist for months or years. While scientific investigations of coseismic landsliding are increasingly common, there is no protocol for rapid (hours-to-days) humanitarian-facing landslide assessment, and no published recognition of what is possible and what is useful to compile immediately after the event. Drawing on the 2015 M_w 7.8 Gorkha earthquake in Nepal, we consider how quickly a landslide assessment based upon manual satellite-based emergency mapping (SEM) can be realistically achieved, and review the decisions taken by analysts to ascertain the timeliness and type of useful information that can be generated. We find that, at present, many forms of landslide assessment are too slow to generate relative to the speed of a humanitarian response, despite increasingly rapid access to high-quality imagery. Importantly, the value of information on landslides evolves rapidly as a disaster response develops, so identifying the purpose, timescales, and end-users of a post-earthquake landslide assessment is essential to inform the approach taken. It is clear that discussions are needed on the form and timing of landslide assessments, and how best to present and share this information, before rather than after an earthquake strikes. In this paper, we share the lessons learned from the Gorkha earthquake, with the aim of informing the approach taken by scientists to understand the evolving landslide hazard in future events and the expectations of the humanitarian community involved in disaster response.

Keywords: Coseismic landslides, Satellite-based emergency mapping, Landslide mapping, Disaster response

1 Introduction

1.1 Mapping landslides after earthquakes

Landsliding is a significant secondary earthquake hazard that can account for up to 25% of earthquake fatalities in mountainous regions (Yin et al., 2009; Budimir et al., 2014). In addition, the collateral damage and disruption caused by landslides substantially inhibits short- and medium-term relief efforts by blocking or destroying transport corridors and communications (Bird and Bommer, 2004; Pellicani et al., 2014; Robinson et al., 2015). The assessment of landslide extent and impacts, beyond direct observations on the ground (Collins and Jibson, 2015; Tiwari et al., 2017), relies on the following three approaches: (1)

empirical modelling, using a combination of pre-earthquake topographic data and information on ground motion and shaking intensity, (2) manual landslide mapping, and (3) automated landslide mapping, both of which use post-earthquake airborne or satellite remote sensing. The main outputs from these assessments are maps of landslide locations, extents and densities, the humanitarian value of which is widely recognized (e.g., Goodchild, 2007).

Each approach has specific data requirements, with the capture and appraisal of those data resulting in an inevitable latency between the event and the release of information (UN-SPIDER, 2015; Fleischhauer et al., 2017). For manual mapping, the speed of information production is influenced by the nature of the landslides themselves, the data quality, and choices about what and how to map (Joyce et al., 2009). Although critical for defining the speed of the assessment, those choices have not previously been described or evaluated with respect to the timescales of the information needs of those on the ground. However, the potential value is clear: if available within a very short timeframe (hours-to-days), information on landsliding can be highly beneficial.

Recently, considerable gains have been made in the capture of satellite imagery used for landslide assessment, particularly in terms of: (1) the resolution and bandwidth of the sensors used; (2) the spatial and temporal coverage; and (3) the ease of access via online repositories (Voigt et al., 2016). However, no single automated method exists to map landslides in rapid response assessments due to the complexities and variability between earthquakes in different locations (Casagli et al., 2016), resulting in uncertainty regarding the type and timeliness of information that is useful to produce. Standards or guidelines for Satellite-based Emergency Mapping (SEM) have been developed for some hazards, such as flooding (UN-SPIDER, 2015; Voigt et al., 2016), but not for landslides. Such guidelines are essential for defining open, constructive and ethical approaches to SEM.

While many satellite operators have tasked rapid image capture of earthquake-affected areas, either on humanitarian grounds via established international frameworks (e.g., the International Charter on Space and Major Disasters), or for commercial ends (Joyce et al., 2009), the use of these data is not necessarily coordinated. For example, commercial satellite imagery at sub-meter resolution was released for the benefit of the response to the 2010 Haiti earthquake (Harp et al., 2011). Over 300 map products were created within two weeks by a plethora of agencies, each using different procedures and standards (UN-SPIDER, 2015; Voigt et al., 2016). Uncoordinated mapping efforts undertaken with different objectives, and for different end-users, can result in a duplication of effort and may cause confusion and data saturation amongst the humanitarian response community. This has the potential to produce an incomplete and inconsistent assessment of humanitarian need (IASC, 2012). In the longer term, these initiatives can result in multiple inventories for the same event, further adding to the confusion. For example, Xu et al. (2014) described 14 separate landslide inventories compiled after the 2008 Wenchuan earthquake in China. After the 2015 Nepal earthquakes, there was a five-fold increase in landslide numbers between the inventories reported by Kargel et al. (2016; 4 312), Martha et al. (2016; 15 551), Roback et al. (2017; 24 915), and Tiwari et al. (2017; 14 670).

1.2 The need for rapid landslide assessment

Despite research defining appropriate scientific methods for coseismic landslide mapping (e.g., Gorum et al., 2011; Harp et al., 2011; Wasowski et al., 2011; Guzzetti et al., 2012), there remains a lack of consideration of the information that is actually

useful for decision makers who are tasked with dealing with an earthquake, particularly where rapid response times are key. Underpinning the effort we describe below is the broad timeframe of a humanitarian disaster response, based upon United Nations disaster response protocols. Central to this is the 'Humanitarian Needs Assessment', which aims to *'provide fundamental information on the needs of affected populations and to support the identification of strategic humanitarian priorities'* (IASC, 2012:4). This approach to disaster response starts immediately after an earthquake and comprises a *Situation Analysis* (completed within 72 hours) and a *Multi-Sector/Cluster Initial Rapid Assessment (MIRA) Report* (completed within two weeks; IASC, 2015). During the first phase, emphasis is placed on obtaining pre- and post-crisis data to determine the disaster extent and scale. This phase '*balances the need for accuracy and detail with the need for speed and timeliness'* (OCHA, 2013) and informs the basis of the mapping approach described below. The UN approach emphasizes the need for information that is fit for purpose, such that superfluous detail and precision are actively discouraged (OCHA, 2013) .

While coseismic landslide inventories created for academic research are slowly and painstakingly collected, this approach is likely to be inconsistent with the requirements for rapid, widespread coverage and the identification of broad areas of concern. The need is therefore to identify the areal extent and location of landsliding (*scale* and *intensity*), assess how landsliding intersects with the location of people and infrastructure (*impacts*), and to appraise the residual risks from induced hazards (*priorities*), such as existing or potential landslide dams. These needs must be balanced against the type and timeliness of information that can be produced. Post-earthquake end-users of landslide information can be numerous, with complex responsibilities, requirements, and information needs. These requirements are also highly dynamic, often shifting from a broad-scale impact assessment to increasingly local level detail over a matter of days, and are therefore challenging to satisfy through SEM (Voigt et al., 2016). As a consequence, the utility of particular forms of information evolves from the initial response to the early recovery. Importantly, the time necessary to produce some forms of information may render them redundant in the context of the initial response, and therefore unnecessary to produce rapidly.

Here we examine these general issues by focussing on the specific case of the 2015 Gorkha earthquake in Nepal. Given the steep terrain, the large rural population, and reported initial shaking intensities in Nepal, the potential for landslide-induced losses as a result of the 2015 earthquakes was quickly recognized (e.g., Gallen et al., 2016; Robinson et al., 2017). We reflect upon a rapid landslide assessment that was undertaken over the first two months after the earthquake, and efforts to disseminate the findings to potential end-users in Nepal. We consider the benefits and time needed for various assessments of landsliding that range from rapid appraisal to a full inventory, enabling an evaluation of the approaches that can effectively inform critical decision making. We also consider the methods that we applied to expedite the generation of usable outputs, which were often at odds with the practices associated with collating a formal scientific landslide inventory. We close by offering recommendations for conducting future humanitarian need-driven rapid landslide assessments following a large earthquake.

Nat. Hazards Earth Syst. Sci. Discuss., https://doi.org/10.5194/nhess-2017-273
Manuscript under review for journal Nat. Hazards Earth Syst. Sci.
Discussion started: 31 July 2017

Natural Hazards and Earth System Sciences Discussions

2 Methods

2.1 Initial landslide identification efforts

Our mapping efforts were undertaken by a group of five analysts with experience of conducting research on landslides in Nepal. The assessments fed information to, and were guided by, the needs of humanitarian actors in Nepal, including the UN Resident Coordinator's Office in Kathmandu and members of the Nepal Risk Reduction Consortium (NRRC), as well as the Cabinet Office Briefing Room (COBR), the Scientific Advisory Group for Emergencies (SAGE), and DFID (Department for International Development) in the UK. Contacts in Nepal were well established because of a long-term collaborative project, Earthquakes without Frontiers (see: ewf.nerc.ac.uk), which brought together natural and social scientists, policy makers, and practitioners with the aim of building societal resilience to earthquakes and associated secondary hazards. These contacts enabled a more rapid assessment of the type of information required during the response. Decisions on how to assess the coseismic landslides invariably related to how and where to map landsliding, and what to map. Based on the need to inform humanitarian response, our assessments focused on the relatively populous middle Himalaya of western and central Nepal, where any landslides were more likely to directly impact people an infrastructure, at the expense of the sparsely populated high Himalaya. This effort ran in parallel to several other initiatives that have subsequently been reported (Kargel et al., 2016; Roback et al., 2017; Tiwari et al., 2017).

The mainshock, which generated the majority of landslides (Martha et al., 2016; Roback et al., 2017), occurred on the Main Himalayan Thrust (MHT) with M_w 7.8 and an epicenter in Gorkha District in Western Nepal. The rupture propagated eastwards, impacting areas up to ~140 km from the epicenter, with additional large aftershocks concentrated near the eastern end of the mainshock rupture plane (Avouac et al., 2015; Galetzka et al., 2015). A rapid appraisal of the first available imagery suggested that landsliding occurred in an E-W swath located north of the Kathmandu Valley, covering a large proportion of Western and Central Nepal (7 500 km^2). Initial indications from coseismic earthquake-triggered landslide models, based on Kritikos et al. (2015) and Parker et al. (2017), were used to direct the mapping effort (see: http://ewf.nerc.ac.uk/2015/04/25/nepal-earthquake-likely-areas-of-landsliding/).

2.2 Data selection

Landslides are most identifiable in optical satellite images under daytime conditions with minimal shadow and cloud, captured at a time of year when vegetation and landslides produce a sharp radiometric contrast. From experience, such conditions are rarely coincident or likely. Landslide inventories conventionally draw on a full catalogue of imagery compiled before mapping begins to ensure consistent coverage of the entire area (Harp et al., 2011). Ideally all images are collected by a single sensor, providing consistent spatial, spectral and radiometric resolution appropriate for the type of landsliding under investigation. A key challenge of time-critical SEM responses is the selection of the most effective imagery for mapping. This selection must be made before complete knowledge of post-earthquake imagery can be acquired, and usually before the general spatial distribution of landsliding is known. Most commonly, imagery from a variety of sensors is captured iteratively, and is

distributed across multiple on- and off-line repositories and platforms. Efficient mapping from this data requires a method for selecting the most 'useful' images, which demands that attributes such as the minimum swath width, maximum topographic distortion, and desired spatial, spectral and radiometric resolutions are defined. The nature of the terrain, the ground cover, and the style of landsliding therefore hold considerable influence over the necessary requirements of imagery that is useful for mapping.

Consequently, as part of our effort, a protocol for prioritizing imagery from which to map was developed (Fig. 1). It quickly became apparent that, given the number and spatial extent of landslides and the need for mapping consistency, beginning to map from a new image committed one mapper for a considerable amount of time. During this time, it was increasingly probable that better imagery of the same area would become available. Imagery was therefore prioritized by three criteria: (1) the platform and hence speed with which the imagery could be handled and analysed; (2) characteristics of the imagery, including cloud cover and geometric distortion; and (3) the spatial and spectral resolution, as well as the swath width. These criteria were used to develop a decision-tree structure for efficient image selection that is described in Fig. 1.

2.2.1 Mapping platform

Efficient mapping requires a platform for quick navigation and mapping of large quantities of images, or a way of bypassing the need for georeferencing. The image source, and hence the platform, influenced which images were prioritized due to the relative ease with which mapping could be conducted as compared to downloading, pre-processing, and mapping from raw imagery. While this made the mapping more fragmented, the mapping time was substantially reduced.

Two platforms were employed: ESRI's ArcMap and Google Earth™. Mapping within ArcMap proved inefficient for several reasons. WorldView-2 and WorldView-3 GeoTIFFs are large files (~1.4 GB panchromatic, ~0.8 GB multi-spectral), required considerable time for pyramid construction, and were hampered by stilted image refresh rates, each of which hindered the speed of mapping. Medium-resolution downsampled JPEGs (~100 MB) were therefore downloaded from the USGS HDDS Explorer as an alternative to increase mapping speed. This reduction in file size equated to a decrease in cell size from ~ 0.3-0.5 m to ~ 3- 4 m, preserving the ability to map most failures. Due to the lack of orthorectification, however, geolocation errors in the JPEG imagery were up to 3 km.

To reduce georeferencing times, we used the DigitalGlobe online platform to view WorldView imagery, running alongside Google Earth™ to view imagery provided by Google Crisis Response, which included DigitalGlobe™ WorldView-2, WorldView-3, and Airbus Pléiades imagery. DigitalGlobe's platform provided the timeliest access to orthorectified WorldView imagery, enabling a rapid assessment of the degree of cloud cover and the extent of landsliding in those areas that had previously been obscured but without the capacity to map onto the images. Access to Google Crisis imagery provided additional benefits: (1) pre-earthquake imagery was readily available to distinguish new and reactivated landslides; (2) image navigation and zooming were quicker than in ArcMap; (3) the capacity for 3D panning and tilting allowed easier identification of landslides; and (4) despite the introduction of geolocation errors (Sato and Harp, 2009), landslides could be digitized and exported into other software.

The use of both ArcMap and Google Earth™ enabled efficient handling of a large array of images of varying extent, resolution and cloud-cover. Google Crisis imagery in Google Earth™ also allowed rapid comparison of multispectral and panchromatic data to identify landslides and better delineate their extent. Despite the relative benefits of Google Crisis, it is important to note that both the georeferencing and orthorectification of imagery were poor owing to image incidence angle and cloud cover. Poor georeferencing made it almost impossible to map by switching between multiple images for a given area of interest, which would otherwise have been a fast and effective mapping strategy. Furthermore, Google Crisis was insufficient as a standalone tool due to geolocation errors and the slow imagery update rate compared to HDDS Explorer. The primary benefit of Google Crisis was the relative ease and speed of operator use, which increased mapping speed once suitable images were available.

2.2.2 Image and sensor characteristics

The second criterion related to the quality of imagery, and was determined primarily by the degree of cloud cover as well as the sensor incidence angle off-nadir. Imagery with minimal cloud cover was prioritized in order to observe as much of the ground as possible within a short period of time and to minimize the time spent on georeferencing. None of the images were completely cloud-free and so mapping was undertaken from multiple images wherever practicable in order to develop a mosaic of coverage. It was especially imperative to distinguish between unmapped areas obscured by cloud cover from mapped areas with no landslides. The angle off-nadir was considered because georeferencing time increased (and accuracy decreased) with increasing angle. Critically for earthquake-triggered landslides, initial data acquisition is commonly focused at the published epicenter, rather than across the full extent of ground shaking. During the initial phases of the response, satellites were tasked to capture images centred on the epicentral region that lay south and west of the most intensive areas of landsliding further to the north. Images to the north and east were therefore captured with relatively high incidence angle off-nadir. This resulted in significant topographic occlusion and image distortion, exacerbated by the steep topography (Roback et al., 2017).

Given the prevalence of cloud cover and off-nadir viewing angles, imagery was drawn upon from a wide range of sensors. With the exception of the EO-1 Advanced Land Imager (ALI) and Landsat 8, the swath width of sensors such as WorldView-2 (16.4 km at nadir) and WorldView-3 (13.1 km at nadir) was small in comparison to the area that experienced shaking sufficient to trigger landsliding (~35 000 km^2), and so large numbers of relatively small-footprint images were needed for complete coverage. Where possible, images with large areal extents were therefore selected to gain a synoptic overview. The time taken to georeference several hundred images, and the varying degrees of success (RMSE of up to ~60-140 m in most areas except for the valley floors), made it unfeasible to process and map imagery fast enough to keep pace with its release. While having a high spatial resolution (~3 m) and short return period, PlanetLabs imagery had a small image footprint (~50 km^2) relative to the affected area (~7 500 km^2). The low radiometric performance of this imagery (Houbourg and McCabe, 2016) also hindered landslide identification in comparison to sensors, such as EO1-ALI.

Spectral resolution and contrast were also used in selecting suitable images. Given our observation that most landslides were shallow and comprised rockfalls and shallow rockslides, spectral resolution and, in particular, the presence of a NIR band were

of considerable importance in landslide mapping. These were prioritized over spatial resolution as long as the latter remained commensurate with the size of landslides. In the case of WorldView-2 and WorldView-3, although panchromatic imagery provides greater spatial resolution, the ability to distinguish vegetation from freshly exposed bedrock and regolith in landslide scars is enhanced using multispectral imagery.

The final criterion was the spatial resolution of imagery. Most large (> 100 m length or width) landslides were observable using the coarsest spatial resolution imagery available (Landsat 8; 30 m visible and NIR but routinely pan-sharpened to 15 m). In catchments with high drainage density, smaller landslides have the potential to block steep, narrow valleys and therefore required very high resolution (VHR; < 2 m) imagery to be delineated. For detailed mapping at a level where the proximity of landslides to infrastructure is important, VHR imagery is also needed. Medium-resolution Landsat 8 imagery, however, still proved useful for two reasons. First, Landsat 8 imagery acquired on 2 May (one week after the mainshock) coincided with widespread cloud-free conditions, providing the first spatially consistent synoptic dataset across the entire affected area. The panchromatic band enabled pan-sharpening of the multispectral data to generate a 15 m resolution image. Pan-sharpening was also undertaken for EO-1 ALI imagery, providing 10 m resolution. Second, the identification of ground control points (GCPs) to align pre- and post-earthquake imagery was more accurate using higher spatial resolution panchromatic imagery. The consistency in the geolocation of WorldView-2 and WorldView-3 multispectral data could therefore be maintained by applying the transformations used in georeferencing the panchromatic data.

2.3 Mapping protocol

For consistency, most landslide inventories adopt a single method of landslide delineation (i.e., as points, polylines, or polygons), depending upon the type of output and the scale of the event. It is also common to identify individual landslides, rather than delineate areas impacted by multiple landslides (Guzzetti et al., 2012; Marc and Hovius, 2015). In global landslide databases (e.g., Kirschbaum et al., 2012; Petley, 2012) and many coseismic landslide inventories, landslides are specified as point features as an efficient means to locate and count large numbers of landslides (Kargel et al., 2016; Tiwari et al., 2017). Regional- to local-scale landslide inventory maps tend to document landslides as polygons, which can be used to understand impact zones or to separate source from deposit (Guzzetti, 2004; Guzzetti et al., 2012). Polygons are required where assessments of sediment yield or connectivity of landslide deposits to the fluvial network are needed (e.g., Roback et al., 2017). The initial focus of our effort was the collection of point data, which was subsequently expanded to polylines. The decision to collect point data was based on the need for rapid analysis and the large numbers (10^3 to 10^4) of landslides, anticipated from previous earthquakes of similar magnitudes. The decision to construct polylines reflected our observation that most of the landslides comprised rockfalls, shallow rockslides, and dry debris flows and avalanches, which often followed pre-existing channels and had highly elongated footprints. The time cost associated with mapping polylines, rather than points, was found to be small relative to the step from points to polygons, while the elongated landslide footprints yielded considerable information on landslide sizes and runout. Our minimum landslide size generally had a major axis of > 50 m. The method

evolved iteratively as data became available and the scale and nature of the landsliding became apparent, the chronology of which is described below.

3 Results

3.1 Chronology of rapid landslide assessment

The chronology of image release, cloud cover, mapping, and released reports is provided in Fig. 2. Within 48 hours of the 25 April mainshock, initial estimates of the likely geographical distribution of landslides were based upon the outputs of the USGS ShakeMap and a limited number of reports from the ground (e.g., via social media). Although this provided a first-order approximation of potential landslide locations, coseismic landsliding is determined by the interactions between topography, ground shaking, and local site geology (Meunier et al., 2008; Marc et al., 2015; Parker et al., 2015). Empirical landslide susceptibility models (Gallen et al., 2016; Parker et al., 2017; Robinson et al., 2017) provided probabilistic estimates of the likelihood of a landslide at any point in space within the affected area. These models predicted that landslide probabilities were high but also variable across the affected districts, especially in the middle to high Himalaya north and east of the epicenter where topographic relief increases, but where population densities remain high. Estimates provided by the USGS ShakeMap, upon which such models rely, underwent several refinements within the first 48 hours, resulting in minor alterations to model predictions, but the overall spatial distribution of relative landslide density remained unchanged. Comparisons between predicted landslide density and observed landslide density have since highlighted some important discrepancies, as discussed by Gallen et al. (2016).

3.3 27 April – 2 May: Direct landslide mapping

Prior to 2 May, cloud cover limited the availability of useable imagery across the entire affected area. During this period, two approaches were undertaken to locate landslides and to prioritise areas for mapping once cloud-free imagery became available. Estimates of landslide location and qualitative size (small/medium/large) were collated from photographs and footage posted on social media and, later, from airborne video from the news media. Although only ~20 landslides were identified and located in this manner, most were in areas north of Kathmandu and at some distance from the epicenter. Secondly, small gaps in cloud cover provided useful indicators of the extent and intensity of landsliding. For example, a small gap in cloud cover of ~1 km^2 in a tributary of the Upper Bhote Kosi Valley in Sindhupalchok District allowed a particularly high number of landslides to be identified in this small area (~25 km^2). This gap in cloud was ~120 km from the epicenter and provided an initial assessment of the nature, type and density of landsliding in the area, as well as verifying the extent of landsliding predicted by landslide models.

Nat. Hazards Earth Syst. Sci. Discuss., https://doi.org/10.5194/nhess-2017-273
Manuscript under review for journal Nat. Hazards Earth Syst. Sci.
Discussion started: 31 July 2017

Natural Hazards and Earth System Sciences Discussions

3.4 After 2 May: Landslide assessment using optical imagery

From 2 May onwards, more frequent small breaks in cloud cover provided useful image coverage in a limited but increasing number of locations. Cloud cover was often concentrated around high elevation topography, leaving valley bottoms visible. Mapping of individual landslides therefore focused in areas proximal to the channel network and lower elevation slopes to survey for landslide dams, similar to those triggered by the 2008 Wenchuan earthquake (Cui et al., 2009).

In order to rapidly map as large an area as possible, and due to cloud cover on higher ground, each landslide was initially marked as a single point at the toe, where the risk to infrastructure and likelihood of valley blocking was greatest. The imagery that was available during this phase had generally high off-nadir viewing angles and so geolocation errors after orthorectification were lower close to valley bottoms. In instances where the landslide toe ran out to but did not block the channel network, a 'yes/no' attribute was added describing the potential for the deposit to block the valley. In instances where upstream pooling of water and a restricted flow downstream was identified indicating blockage, a separate valley-blocking marker was created (Fig. 3). These locations were fed to the USGS for visual inspection as part of their assessment of present and future landslide hazards (Collins and Jibson, 2015).

Valleys with particularly intense landsliding were recorded with a polyline running up river from the southernmost visible extent of landsliding (Fig. 3). The aim of this was to delineate the southernmost limit of major landslide disruption, and hence the likely northern limit of unimpeded road access, using the predominantly north – south oriented drainage network. This was mapped as a solid line where the limit was observed and a dashed line where the limit was inferred in the absence of imagery. Subsequent mapping showed this line to be an accurate estimate. A map containing this information was released on 4 May, approximately two days after cloud cover reduced and nine days after the mainshock (Fig. 3).

As increasingly cloud-free imagery became available (cf. Roback et al., 2017), manual mapping speeds increased. Landslides were subsequently identified with polylines to provide an attribute of scale and to define where landslides intersected infrastructure, such as roads. A record of areas mapped and areas obscured by cloud was maintained. Mapping using VHR imagery identified that the majority of coseismic landslides were narrow (~ 10 m) and hence would be difficult to identify in lower resolution imagery. Updated maps were published online on 7 May (Fig. 4) and 21 May (Fig. 5), which featured both increasing numbers and coverage of landslides.

Our accompanying notes (see, for example, Table 1) summarised the key observations, the methods used, and key messages about the intensity, locations and general risks posed by these landslides. The maps and underpinning data were disseminated as Google Earth™ KML files and ArcGIS shapefiles on the Humanitarian Data Exchange Nepal (https://data.humdata.org/group/nepal-earthquake). In addition, *.PDF versions of district-level landslide maps in colour and black and white, alongside interpretive notes in English and Nepali, were posted on the Earthquakes without Frontiers blog (http://ewf.nerc.ac.uk/2015/05/28/nepal-updated-28-may-landslide-inventory-following-25-april-nepal-earthquake/) and the National Society for Earthquake Technology website (http://www.nset.org.np/eq2015/), as well as being sent directly to the

UN RCO and Nepal Red Cross. This information was later used in, for example, UN-led monsoon preparedness planning, and by the military in their assessment of road access constraints (Datta et al., forthcoming).

Approximately 5 600 coseismic landslides were identified in the affected area by 18 June, 42 days after the earthquake. This comprised ~4 500 triggered by the 25 April Gorkha earthquake, ~300 by the 12 May Dolakha earthquake, and ~800 that could be attributed to either event. Some areas remained obscured by clouds throughout this period and were therefore recorded as such in our final map (Fig. 6).

4 Discussion

4.1 Comparison of landslide mapping

Comparing our rapidly-derived inventory with subsequent, independently collated inventories (Martha et al., 2016; Roback et al., 2017; Tiwari et al., 2017) shows that our inventory underestimated the total number of landslides by up to ~ 19 000. However, the spatial pattern and relative intensity closely adheres to those described in both Martha et al. (2016) and Roback et al. (2017). The inventory therefore holds value as a rapid assessment of the relative intensity of landsliding and its spatial distribution, and as a tool for identifying the worst affected areas. This raises questions about the value of the time investment necessary to rapidly assess absolute landslide numbers and volumes, or the maximum extent of landsliding, as useful metrics for informing earthquake disaster response. Below, we discuss the utility of such metrics in terms of the benefit of the extra detail they provide compared to the increased time required to derive them. This is an attempt to identify and develop common standards for rapid SEM for landslide-triggering events that can effectively inform humanitarian response.

4.2 Can manual landslide mapping provide useful information quickly enough to inform humanitarian response efforts?

Generating a useful assessment of landsliding immediately after an earthquake remains challenging due to a lack of clarity around what information is possible to acquire under severe time constraints, and what information is actually useful (Robinson et al., 2017). Our mapping effort showed that delays in information production can occur due to: image availability, image quality, cloud cover, and the time taken to handle and map from imagery once it became available. While some clarity on increasing the speed of these processes can be provided via reflections such as this, pertinent information is inevitably unique to each earthquake and its socio-political context. At the highest level, information on landsliding within the first 72 hours can help to define the scale, extent, and distribution of landslide impacts across the entire affected area, particularly if this area is otherwise. Given the delays in image capture and mapping, full landslide mapping for an event on the scale of the Gorkha earthquake or larger is impossible to achieve within this 72-hour timeframe. However, as the number and exact location of all landslides is not important to disaster managers at this stage of a response (OCHA, 2013; IASC, 2015), a faster approach is preferable.

Robinson et al. (2017) explored the merits of seeding an empirical landslide with the initial outputs from rapid post-earthquake mapping efforts, such as our initial attempts (Fig. 3). They found that small numbers (~10^2) of mapped landslides were sufficient to accurately predict the spatial hazard posed by ~10^4 landslides across the entire affected area, and we have shown that such small numbers of landslides can be mapped within the 72-hour timeframe. Importantly, however, when models and empirical data are presented together, their relative merits and drawbacks need to be clearly articulated. For example, while models can suggest where landsliding is more or less likely to have occurred with varying degrees of certainty, direct observations provide absolute certainty at some locations, but remain inherently uncertain where the ground has not been observed. Conversely, combining models and observations to draw conclusions about the likely presence of landslides where the ground has yet to be observed may enable faster dissemination of information to end-users where full mapping is not practicable. Using gaps in the initial cloud cover, our identification of valleys of severe landsliding and prediction of the southernmost extent of landsliding was achieved within two days of images becoming available. This highlights the importance of nested monitoring within SEM (Voigt et al., 2016) whereby coarser imagery with large footprints can be used to identify areas of concern, which can be subsequently monitored using higher resolution approaches.

A clear exception to this finding is in assessing the imminent potential for secondary hazards posed by landslide dams (e.g., Cui et al., 2009; Kargel et al., 2016). It is widely recognised that landslide dams typically fail soon after formation, with 41% failing within one week (Costa and Schuster, 1987). Rapid assessment to inform the management of this risk is therefore vital. However, features indicative of progressive failure, such as widening tension cracks, are too small to be visible in even the highest resolution satellite imagery, and so SEM is mostly valuable for locating and low-resolution monitoring of landslide dams. An appraisal of the risk that they pose is best undertaken on the ground.

Our findings suggest that there is potential additional value in informing post-earthquake landslide mapping efforts to target medium to longer-term information needs, rather than the immediate response. The transition from disaster response to recovery can occur over a matter of days, and while some information gathered in the immediate earthquake aftermath may not be instantly useful, it may become valuable for later decision. For example, given that earthquakes elevate landslide hazard for sustained periods of time (e.g. Marc et al., 2015), continually updating coseismic landslide maps to assess how the hazard evolves is potentially of great value, yet is rarely undertaken. In the aftermath of the Nepal earthquake, there were 46 days between the mainshock and the first rainfall-induced fatal landslide of the monsoon. Detailed mapping that describes individual landslides and the potential for remobilization is invaluable in assessing risks during future monsoons. However, as such uses require a high level of local detail and precision, mapping must be accurate, which can be difficult to achieve within limited timeframes. Defining the aim and output of responsive mapping is therefore vital to establish the data that must be collected.

It is equally clear that there is no requirement to wait until an earthquake occurs to start defining what information could be useful with those charged with managing the response. Scenarios or planning exercises are widely used to prepare those involved in disaster response (Davies et al., 2015), and could be extended to consider coseismic landslide hazard assessments, to define what information can be provided and when. This process would be of value to end-users, but also to those producing landslide assessments to ensure that aims are realistic and defined by needs. Similar discussions for other forms of geohazard

have benefitted from protocols and guidelines that aim to standardize approaches, outputs and procedures (UN-SPIDER, 2015). Groups such as the CEOS Working Group on Disasters, and the UN-SPIDER IWG-SME, are vital frameworks for establishing these technical, practical and ethical guidelines on SEM for coseismic landslide assessment.

4.3 The best way to map coseismic landslides?

In circumstances where mapping individual landslides is of value, the choice of whether to digitize points, polylines or polygons is an important consideration. The choice must be based on the extent of the mapping area but also on the desired outputs and the scale at which they will be used. The reliability of the geometrical data provided by polygons, while beneficial, is highly sensitive to the accuracy and consistency of image orthorectification, which are challenging in steep terrain. We observed that, where a landslide spanned an altitudinal range of more than several hundred metres, the accuracy of results generated strongly depended upon the spatial resolution of the imagery and the sensor incidence angle. As a result, where multiple data sources are used and image resolution varies across the affected area, the number and size distributions of polygons also vary, leading to systematic inconsistencies in mapping. Coarser, and hence more rapid, methods of mapping are valuable for a rapid assessment of landslide impact across the whole earthquake affected area, but are less useful for understanding individual landslides. We found that polylines offered a compromise that retains some of the speed of mapping points, but also enables an assessment of landslide size and intersection with features of interest, such as roads, buildings, or rivers.

Automated and semi-automated identification methods hold potential for rapid landslide mapping, with potential benefits over manual methods that increase with the total area affected. These methods tend to draw on very high resolution imagery, and can be broadly divided into pixel-by-pixel change detection (e.g., Tsai et al., 2010; Mondini et al., 2011; Stumpf and Kerle, 2011) and object-based change detection (e.g., Barlow et al., 2006; Moine et al., 2009; Martha et al., 2010). Both methods rely on pre- and post-earthquake differences in the spectral values, most often using ratio derivatives such as NDVI, and the image spectral angle derived from blue, green, red, and near-infrared values. While these data can be readily available, the results are susceptible to large spectral variance between pixels, and are sensitive to coregistration errors (Stumpf and Kerle, 2011). The results can also be highly sensitive to image pre-processing, including pan-sharpening, atmospheric correction, and orthorectification (Mondini et al., 2011). Furthermore, the use of automated and semi-automated methods relies upon discernible changes in the spectral response, which are highly dependent on landslide character. While these approaches have been undertaken following previous earthquakes and heavy rainfall (e.g., Tsai et al., 2010), their utility in post-disaster humanitarian response remains reliant upon future research (Voigt et al., 2016).

4.4 What limits the time needed to produce a useful landslide assessment?

The time taken to produce outputs from our mapping campaign was most influenced by image availability, specifically that which was cloud free over the area of interest. For this earthquake, the workload of five analysts appeared to yield a suitable balance between capacity, shared learning, and consistency, given the timeframes to produce outputs. It was beneficial for all

mappers to be in one laboratory, enabling easy coordination and communication to ensure coverage and consistency and to avoid replication. We were able to partition the earthquake-affected area into regions of interest for each mapper, and these regions were dynamically updated in response to the availability of high(er) quality imagery. Given the increased capacity of the SEM community to develop map products in recent years, this partitioning represents an important phase in the coordination of multiple groups, thereby avoiding repetition and increasing the consistency of outputs (Voigt et al., 2016).

The introduction of larger satellite constellations with more advanced sensors also expedites the availability of imagery for future mapping campaigns, increasing the efficiency of post-disaster mapping (Voigt et al., 2016). For example, Sentinel-2a combines a large swath-width (290 km) with a moderately high spatial resolution (10 m visible and near-infrared), which will reduce the number of images, and thus processing time, required to cover large areas. In addition, the higher return frequency (10 days for Sentinel-2a, compared to 16 days for Landsat 8) will increase the probability of observing the ground through gaps in cloud cover, reducing the time needed to produce outputs. Sentinel-2b is expected to decrease the return period further to five days. Our effort demonstrated that once imagery is available, mapping can be rapid (two to three days), given suitable capacity.

The timeliness of an SEM landslide assessment must be considered relative to alternative sources of information. While each earthquake is different, multiple sources of information will become available to decision makers, primarily based upon networks collating human intelligence from those on the ground. In Nepal, nationwide systems capable of rapidly assessing the earthquake impacts included the networks of the military, Red Cross, and local government. Such approaches can, however, be subjective, incomplete and inconsistent in coverage, and cumbersome to administer (OCHA, 2013; Datta et al., forthcoming). Inevitably, such assessments are also restricted to areas with functioning communications or to accessible parts of the road network, at least until systematic reconnaissance can be undertaken. Such systematic reconnaissance is also highly contingent upon favourable weather and available resources. Consequently, some areas can remain isolated for days or weeks. For example, the Jhelum Valley in Pakistan after the 2005 Kashmir earthquake (Petley et al., 2006; Owen et al., 2008; Mahmood et al., 2015) and the Rasuwa and Upper Bhote Kosi valleys after the 2015 Nepal earthquakes were left isolated by landsliding, leaving the status of thousands of households largely unknown as the wider response effort gained pace.

4.5 Science, citizen science, and coseismic landslide assessment

Through the proliferation of mobile technologies, open-source mapping, and online GIS, an increasingly important role for social media and crowd-sourced data in disaster response is emerging (e.g., Zook et al., 2010; Fleischhauer et al., 2017). Crowd-sourced mapping campaigns initiated by Tomnod (with imagery from DigitalGlobe™) and OpenStreetMap (with imagery from Airbus) provided users with access to image tiles and the ability to create and edit vectorized shapes. These sites produced damage maps that were used extensively by the Nepali military, both for logistics planning and for identifying communities in need of assistance (The Nepalese Army, 2015). The value of such crowd-sourced information has also been recognized by the scientific community in response to several recent natural disasters (e.g. Goodchild and Glennon, 2010; Barrington et al., 2012; Roche et al., 2013; Poiani et al., 2016).

To date crowd sourcing has not, however, been employed to map coseismic landslides in a manner that is reliable. Landslide mapping requires pre- and post-earthquake datasets, knowledge of failure processes and mechanics, and an understanding of what is possible to observe based on the spectral characteristics of the imagery. Research is needed into how best to support crowd-sourced mapping to generate reliable landslide mapping and inventories, and to feed learning from compiling science-focussed landslide inventories into this process. In our campaign, we also benefited from insights from social media to identify and locate landslides in areas with persistent cloud cover. A combination of archived pre-earthquake imagery and reported locations allowed us to locate the exact hillslope that had failed in 20 locations, the positions of which were later verified by our formal mapping. A platform that permits this combination of data with more conventional mapping therefore offers an attractive means of collating and verifying landslide data.

Advances in collating landslide inventories, including crowd-sourcing, and the key messages that can be distilled from their analysis, are valuable for disaster response. However, key messages need to be articulated quickly and clearly along with any associated limitations or uncertainties. The various means of landslide assessment that have been discussed above are summarised in Table 2. This provides a chronology of outputs that clarifies what we have found possible to achieve within the timeframes of the UN Situation Analysis and MIRA report. While the timescales of what is possible will vary between events (for landslide mapping, predominantly as a function of cloud cover), the benefits and limitations of each are included to provide detail on what is and is not possible to conclude. Importantly, once a dataset is made available online, it is publicly available for the foreseeable future. While this provides a good base for others to work from, care is needed in how and where data are shared and how caveats and uncertainties are communicated, in particular the method used to generate the dataset. Based on our experience of communicating landslide assessments, each published output requires the following accompanying information: (1) a supporting narrative that describes the aims, assumptions, methods, and limitations of the data; (2) a high-level analysis of the key messages or conclusions that can and cannot be reached on the basis of the mapping; (3) a statement of intent for further work, so that end-users can see how the work will evolve; and (4) a mechanism for feedback or exchange between mappers and end-users. Unless these elements are made available, the output is likely to be either overlooked, or it may be used in ways which were not intended.

5 Conclusions

In this paper we have reflected on our experience of creating an inventory of coseismic landslides rapidly after the 2015 Nepal earthquakes. While scientific efforts to map coseismic landslides may aim to assess the hazard in an urgent manner to inform the humanitarian response, they are rarely completed rapidly enough to do so. As such, scientific efforts to generate useful information require recognition of what is both useful and practicable within the available timeframe. We have demonstrated what can realistically be achieved, including the time critical decisions that need to be taken to expedite the mapping process. While any increase in the rate of image availability increases the likelihood of producing useful landslide assessments, the

consideration of what is possible (given handling and processing constraints on mapping) and what is useful (given the priorities of end-users responding to humanitarian crises) remains pertinent for other future events.

Our lessons can and should inform the approach and expectations of those who seek to produce rapid (days to months) coseismic landslide assessments, and those who would benefit from using this information. There is clearly no requirement to wait until an earthquake occurs to begin conversations around what is or could be useful, and these conversations should involve scientists, government representatives, and humanitarian response teams. The efforts of UN-SPIDER and the CEOS Disaster Working Group are vital for ensuring coherence in the response to future earthquakes. With rapid advances in social media and accessible geospatial data, it is likely that future post-earthquake assessment will benefit from more systematic crowd-sourced data collection and integration.

References

Avouac, J.-P., Meng, L., Wei, S., Wang, T. and Ampuero, J.-P.: Lower edge of locked Main Himalayan Thrust unzipped by the 2015 Gorkha earthquake, Nat. Geosci., 8(9), 708–711, doi:10.1038/ngeo2518, 2015.

Barrington, L., Ghosh, S., Greene, M., Har-Noy, S., Berger, J., Gill, S., Lin, A. and Huyck, C.: Crowdsourcing earthquake damage assessment using remote sensing imagery, Ann. Geophys, 54(6) [online] Available from: http://www.annalsofgeophysics.eu/index.php/annals/article/view/5324, 2012.

Bird, J. and Bommer, J.: Earthquake losses due to ground failure, Eng. Geol., 75(2), 147–179, doi:10.1016/j.enggeo.2004.05.006, 2004.

Budimir, M., Atkinson and Lewis: Earthquake-and-landslide events are associated with more fatalities than earthquakes alone, Nat. Haz., 72(2), 895–914, doi:10.1007/s11069-014-1044-4, 2014.

Casagli, N., Cigna, F., Bianchini, S., Hölbling, D., Füreder, P., Righini, G., Del Conte, S., Friedl, B., Schneiderbauer, S., Iasio, C., Vlcko, J, Greif, V., Proske, H., Granica, K., Falco, S., Lozzi, S., Mora, O., Arnaud, A., Novali, F., and Bianchi, M.: Landslide mapping and monitoring by using radar and optical remote sensing: examples from the EC-FP7 project SAFER, P-Soc. Photo-Soc. Env., 4, 92–108, doi:10.1016/j.rsase.2016.07.001, 2016.

Collins, B. and Jibson, R.: Assessment of existing and potential landslide hazards resulting from the April 25, 2015 Gorkha, Nepal earthquake sequence, No. 2015-1142, US Geological Survey, doi:10.3133/ofr20151142, 2015.

Costa, J. E. and Schuster, R. L.: The formation and failure of natural dams, Geol. Soc. Am. Bull., 100(7), 1056-1068 1987.

Cui, P, Zhu, Y, Han, Y, Chen, X and Zhuang, J: The 12 May Wenchuan earthquake-induced landslide lakes: distribution and preliminary risk evaluation, Landslides, 6(3), 209-223, doi: 10.1007/s10346-009-0160-9, 2009.

Datta, A., Oven, K.J., Rosser, N.J., Sigdel, A., Densmore, A.L. and Rigal, S.: The use of scientific evidence during the 2015 Nepal earthquake, Overseas Development Institute (London) Working Paper, forthcoming.

Davies, T., Beaven, S., Conradson, D., Densmore, A., Gaillard, J.C., Johnston, D., Milledge, D., Oven, K., Petley, D., Rigg, J. and Robinson, T.: Towards disaster resilience: A scenario-based approach to co-producing and integrating hazard and risk knowledge, Int. J. Disaster Risk Re., 13, 242-247, 2015.

Duda, K.A. and Jones, B.K.: USGS remote sensing coordination for the 2010 Haiti earthquake, P. Eng. Remote Sensing, 77(9), 899-907, doi: 10.14358/PERS.77.9.899, 2011.

Đurić, D., Mladenović, A., Pešić-Georgiadis, M., Marjanović, M. and Abolmasov, B.,: Using multiresolution and multitemporal satellite data for post-disaster landslide inventory in the Republic of Serbia, Landslides, 1-16, doi: 10.1007/s10346-017-0847-2, 2017.

ECHO: Crisis Falsh No. 10, European Commision Humanitarian Aid and Civil Protection Report, available from: http://www.europarl.europa.eu/meetdocs/2014_2019/documents/deve/dv/echo_crisis_flash_10_nepal_earthquake_/echo_crisis_flash_10_nepal_earthquake_en.pdf, 2015.

Fleischhauer, S., Behr, F.-J., and Rawiel, P.: Concept and implementation of an architecture for the immediate provision of geodata in disaster management, Int. Arch. Photogramm. Remote Sens. Spatial Inf. Sci., XLII-4/W2, 73-78, https://doi.org/10.5194/isprs-archives-XLII-4-W2-73-2017, 2017.

Galetzka, J., Melgar, D., Genrich, J.F., Geng, J., Owen, S., Lindsey, E.O., Xu, X., Bock, Y., Avouac, J.P., Adhikari, L.B. and Upreti, B.N.: Slip pulse and resonance of the Kathmandu basin during the 2015 Gorkha earthquake, Nepal, Science, 349(6252), 1091-1095, doi: 10.1126/science.aac6383, 2015.

Gallen, S.F., Clark, M.K., Godt, J.W., Roback, K. and Niemi, N.A.: Application and evaluation of a rapid response earthquake-triggered landslide model to the 25 April 2015 M_w 7.8 Gorkha earthquake, Nepal, Tectonophysics, doi: 10.1016/j.tecto.2016.10.031, 2016.

Goodchild, M. F.: Recognition of GIS critical, GIM International, 21(4), 431, 2007.

Goodchild, M. and Glennon, A.: Crowdsourcing geographic information for disaster response: a research frontier, Int. J. Digital Earth, 231–241, doi:10.1080/17538941003759255, 2010.

Gorum, T., Fan, X., van Westen, C., Huang, R., Xu, Q., Tang, C. and Wang, G.: Distribution pattern of earthquake-induced landslides triggered by the 12 May 2008 Wenchuan earthquake, Geomorphology, 133(3-4), 152–167, doi:10.1016/j.geomorph.2010.12.030, 2011.

Guzzetti, F, Mondini, AC, Cardinali, M and Fiorucci, F: Landslide inventory maps: New tools for an old problem, Earth Sci. Rev., 112(1), 42-66, doi: 10.1080/17445647.2014.949313, 2012.

Guzzetti, F.: Landslide hazard and risk assessment, Ph.D. Thesis, University of Bonn, 2004.

Harp, E., Keefer, D., Sato, H. and Yagi, H.: Landslide inventories: The essential part of seismic landslide hazard analyses, Eng Geol, 122(1-2), 9–21, doi:10.1016/j.enggeo.2010.06.013, 2011.

Hölbling, D., Eisank, C., Albrecht, F., Vecchiotti, F., Friedl, B., Weinke, E. and Kociu, A.: Comparing Manual and Semi-Automated Landslide Mapping Based on Optical Satellite Images from Different Sensors, Geosciences, 7(2), 37, doi: 10.3390/geosciences7020037, 2017.

Houbourg, R. and McCabe, M.F.: High-Resolution NDVI from Planet's Constellation of Earth Observing Nano-Satellites: A New Data Source for Precision Agriculture, Remote Sens., 8, 786-804, doi: 10.3390/rs8090768, 2016.

IASC: Multi-sector initial rapid assessment guidance (MIRA), Inter-Agency Standing Committee, available from: https://docs.unocha.org/sites/dms/documents/mira_final_version2012.pdf, 2012.

IASC: Multi-sector initial rapid assessment guidance, Inter-Agency Standing Committee, available from: https://www.humanitarianresponse.info/en/programme-cycle/space/document/multi-sector-initial-rapid-assessment-guidance-revision-july-2015, 2015.

Joyce, K., Belliss, S., Samsonov, S., McNeill, S. and Glassey, P.: A review of the status of satellite remote sensing and image processing techniques for mapping natural hazards and disasters, Prog. Phys. Geog., 33(2), 183–207, doi:10.1177/0309133309339563, 2009.

Kargel, J.S., Leonard, G.J., Shugar, D.H., Haritashya, U.K., Bevington, A., Fielding, E.J., Fujita, K., Geertsema, M., Miles, E.S., Steiner, J., Anderson, E., Bajracharya S., Bawden G.W., Breashears D.F., Byers A., Collins, B., Dhital, M.R., Donnellan, A., Evans T.L., Geai M.L., Glasscoe, M.T., Green, D., Gurung, D.R., Heijenk, R., Hilborn, A., Hudnut, K., Huyck, C., Immerzeel, W.W., Liming, J., Jibson, R., Kääb, A., Khanal, N.R., Kirschbaum, D., Kraaijenbrink, P.D.A, Lamsal, D., Shiyin, L., Mingyang, L., McKinney, D., Nahirnick, N.K., Zhuotong, N., Ojha, S., Olsenholler, J., Painter, T.H., Pleasants, M., Pratima, K.C., Yuan, Q.I., Raup, B.H., Regmi, D., Rounce, D.R., Sakai, A., Donghui, S., Shea, J.M., Shrestha, A.B., Shukla, A., Stumm, D., van der Kooij, M., Voss, K., Xin, W., Weihs, B., Wolfe, D., Lizong, W., Xiaojun, Y., Yoder, M.R. and Young, N.: Geomorphic and geologic controls of geohazards induced by Nepal's 2015 Gorkha earthquake, Science, 351(6269), aac8353, doi:10.1126/science.aac8353, 2016.

Kirschbaum, D., Adler, R., Adler, D., Peters-Lidard, C. and Huffman, G., Global distribution of extreme precipitation and high-impact landslides in 2010 relative to previous years, J. Hydrometeorology, 13(5), 1536-1551, doi: 10.1175/JHM-D-12-02.1, 2012.

Kritikos, T., Robinson, T. R. and Davies, T. R.: Regional coseismic landslide hazard assessment without historical landslide inventories: A new approach, J. Geophys. Res.-Earth Surf., 120(4), 711-729, doi:10.1002/2014JF003224, 2015.

Mahmood, I., Kidwai, A., Qureshi, S., Iqbal, M. and Atique, L.: Revisiting major earthquakes in Pakistan, Geology Today, 33–38, doi:10.1111/gto.12085, 2015.

Lu, P., Stumpf, A., Kerle, N. and Casagli, N.: Object-oriented change detection for landslide rapid mapping. IEEE Geosci. Remote. Sens. Lett., 8(4), 701-705, doi: 10.1109/LGRS.2010.2101045, 2011.

Marc, O., Hovius, N., Meunier, P., Uchida, T. and Hayashi, S.: Transient changes of landslide rates after earthquakes, Geology, doi:10.1130/G36961.1, 2015.

Marc, O. and Hovius, N.: Amalgamation in landslide maps: effects and automatic detection, Nat. Haz. Earth Sys., 15(4), 723–733, doi:10.5194/nhess-15-723-2015, 2015.

Marc, O., Hovius, N., Meunier, P., Gorum, T. and Uchida, T.,: A seismologically consistent expression for the total area and volume of earthquake-triggered landsliding, J. Geophys. Res.: Earth Surf., 121(4), 640-663, doi: 10.1002/2015JF003732, 2016.

Martha, T.R., Kerle, N., Jetten, V., van Westen, C.J. and Kumar, K.V.: Characterising spectral, spatial and morphometric properties of landslides for semi-automatic detection using object-oriented methods, Geomorphology, 116(1), 24-36, doi: 10.1016/j.geomorph.2009.10.004, 2010.

Martha, T., Roy, P., Mazumdar, R., Govindharaj, B. and Kumar, V.: Spatial characteristics of landslides triggered by the 2015 M_w 7.8 (Gorkha) and M_w 7.3 (Dolakha) earthquakes in Nepal, Landslides, 14(2), 697–704, doi: 10.1007/s10346-016-0763-x, 2016.

Meunier, P., Hovius, N. and Haines, J.: Topographic site effects and the location of earthquake induced landslides, Earth Planet Sc. Lett., 275(3-4), 221–232, doi:10.1016/j.epsl.2008.07.020, 2008.

Mondini, A. C., Guzzetti, Reichenbach, Rossi, Cardinali and Ardizzone: Semi-automatic recognition and mapping of rainfall induced shallow landslides using optical satellite images, Remote Sens. Env., 115(7), 1743-1757, doi: 10.1016/j.rse.2011.03.006, 2011.

OCHA: United Nations Disaster Assessment and Coordination, United Nations Office for the Coordination of Humanitarian Affairs, 2013.

Owen, L., Kamp, U., Khattak, G., Harp, E., Keefer, D. and Bauer, M.: Landslides triggered by the 8 October 2005 Kashmir earthquake, Geomorphology, 94(1-2), 1–9, doi:10.1016/j.geomorph.2007.04.007, 2008.

Parker, R.N., Hancox, G.T., Petley, D.N., Massey, C.I., Densmore, A.L. and Rosser, N.J.: Spatial distributions of earthquake-induced landslides and hillslope preconditioning in the northwest South Island, New Zealand, Earth Surf. Dynam., 3(4), 501, doi: 10.5194/esurf-3-501-2015, 2015.

Parker, R., Rosser, N. and Hales, T.: Spatial prediction of earthquake-induced landslide probability, Nat. Haz. Earth Syst., 1–29, doi:10.5194/nhess-2017-193, 2017.

Pellicani, R., Westen, C. and Spilotro, G.: Assessing landslide exposure in areas with limited landslide information, Landslides, 11(3), 463–480, doi:10.1007/s10346-013-0386-4, 2014.

Petley, D.: Global patterns of loss of life from landslides, Geology, 40(10), 927–930, doi:10.1130/G33217.1, 2012.

Petley, D., Dunning, S., Rosser, N. and Kausar, A.: Incipient landslides in the Jhelum Valley, Pakistan following the 8th October 2005 earthquake, in: Disaster Mitigation of Debris Flows, Slope Failures and Landslides, Frontiers of Sci. Ser., University Academy Press, Tokyo, Japan, 47-56, 2006.

Poiani, T., dos Rocha, S. R. and Degrossi, L. C.: Potential of collaborative mapping for disaster relief: A case study of OpenStreetMap in the Nepal earthquake 2015, 49th Hawaii International Conference on System Sciences, 6-7 January 2016, 188-197, 2016.

Roback, K, Clark, MK, West, AJ, Zekkos, D and Li, G: The size, distribution, and mobility of landslides caused by the 2015 M_w 7.8 Gorkha earthquake, Nepal, Geomorphology, doi: 10.1016/j.geomorph.2017.01.030, 2017.

Robinson, T., Davies, T., Wilson, T., Orchiston, C. and Barth, N.: Evaluation of coseismic landslide hazard on the proposed Haast-Hollyford Highway, South Island, New Zealand, Georisk: Assessment and Management of Risk for Engineered Systems and Geohazards, 10(2), 146–163, doi:10.1080/17499518.2015.1077974, 2015.

Robinson, T., Rosser, N., Densmore, A., Williams, J., Kincey, M., Benjamin, J. and Bell, H.: Rapid post-earthquake modelling of coseismic landslide magnitude and distribution for emergency response decision support, Nat. Haz. Earth Sys., 1–29, doi: 10.5194/nhess-2017-83, 2017.

Roche, S, Propeck-Zimmermann, E and Mericskay, B: GeoWeb and crisis management: Issues and perspectives of volunteered geographic information, GeoJournal, 78(1), 21-40, doi: 10.1007/s10708-011-9423-9, 2013.

Sato, H.P. and Harp, E.L.: Interpretation of earthquake-induced landslides triggered by the 12 May 2008, M7.9 Wenchuan earthquake in the Beichuan area, Sichuan Province, China using satellite imagery and Google Earth, Landslides, 6(2), 153–159, doi:10.1007/s10346-009-0147-6, 2009.

Stumpf, A. and Kerle, N.: Object-oriented mapping of landslides using Random Forests, Remote Sens. Env., 115(10), 2564–2577, doi:10.1016/j.rse.2011.05.013, 2011.

The Nepalese Army: The Nepalese Army in the Afternamth of the Gorkha Earthquake of 2015 - Experiences and lessons learned. Publication of the Nepalese Army, Kathmandu, 52 pp., 2015.

Tiwari, B, Ajmera, B and Dhital, S: Characteristics of moderate-to large-scale landslides triggered by the M_w 7.8 2015 Gorkha earthquake and its aftershocks, Landslides, doi: 10.1007/s10346-016-0789-0, 2017.

Tsai, F., Hwang, J.-H., Chen, L.-C. and Lin, T.-H.: Post-disaster assessment of landslides in southern Taiwan after 2009 Typhoon Morakot using remote sensing and spatial analysis, Nat. Haz. Earth Sys., 10, 2179–2190, doi:10.5194/nhess-10-2179-2010, 2010.

UN-SPIDER: Emergency mapping guidelines, International Working Group on Satellite-based Emergency Mapping (IWG-SEM), 2015.

Voigt, S., Giulio-Tonolo, F., Lyons, J., Kučera, J., Jones, B., Schneiderhan, T., Platzeck, G., Kaku, K., Hazarika, M.K., Czaran, L. and Li, S.: Global trends in satellite-based emergency mapping, Science, 353(6296), 247-252, doi: 10.1126/science.aad8728, 2016.

Wasowski, J., Keefer, D. and Lee, C.-T.: Toward the next generation of research on earthquake-induced landslides: Current issues and future challenges, Eng. Geol., 122(1-2), 1–8, doi: 10.1016/j.enggeo.2011.06.001, 2011.

Xu, C., Shyu, J.B.H. and Xu, X., 2014. Landslides triggered by the 12 January 2010 Port-au-Prince, Haiti, M_w= 7.0 earthquake: visual interpretation, inventory compiling, and spatial distribution statistical analysis, Nat. Haz. Earth Sys., 14(7), 1789, doi: 10.5194/nhess-14-1789-2014, 2014.

Yin, Y., Wang, F. and Sun, P.: Landslide hazards triggered by the 2008 Wenchuan earthquake, Sichuan, China, Landslides, 6(2), 139–152, doi: 10.1007/s10346-009-0148-5, 2009.

Zook, M, Graham, M and Shelton, T: Volunteered geographic information and crowdsourcing disaster relief: a case study of the Haitian earthquake, World Medical and Health Policy, 2(2), 7-33, doi: 10.2202/1948-4682.1069, 2010.

Nat. Hazards Earth Syst. Sci. Discuss., https://doi.org/10.5194/nhess-2017-273
Manuscript under review for journal Nat. Hazards Earth Syst. Sci.
Discussion started: 31 July 2017

Natural Hazards and Earth System Sciences Discussions

Tables

Table 1: Example of notes that accompanied the map released on 18th June, an extract from which is presented in Fig. 6.

The Dolakha aftershock on 12 May (15 days after the 25 April mainshock) prompted a second campaign of mapping in response to reports of further landslides close to its epicenter. In the week following 12 May, most new optical imagery was acquired with incidence angles of 25-45°. Given the extreme relief in the epicentral region, it was decided to delay mapping until more suitable imagery became available. A landslide map derived from imagery collected after both earthquakes was therefore not released until 18 June (54 days after the mainshock), with landslides categorised as follows:

(1)	Failures positively identified as occurring as a result of the 25 April Gorkha earthquake
(2)	Failures positively identified as occurring as a result of the 12 May Dolakha earthquake
(3)	Failures that occurred *either* as a result of the 25 April Gorkha earthquake *or* 12 May Dolakha earthquake, having occurred in areas where cloud-free imagery was only available after 12 May.
(4)	Failures considered likely to have been caused by either the Gorkha *or* Dolakha earthquake, but where pre-earthquake imagery was only available prior to the 2014 monsoon season.
(5)	Landslides that had been observed after the 25 April Gorkha earthquake but which had not changed after the 12 May Dolakha earthquake

Nat. Hazards Earth Syst. Sci. Discuss., https://doi.org/10.5194/nhess-2017-273
Manuscript under review for journal Nat. Hazards Earth Syst. Sci.
Discussion started: 31 July 2017

Natural Hazards and Earth System Sciences
Discussions

Table 2: Timescales, benefits, and limitations of landslide-related outputs, based on response to a large continental earthquake in a mountainous region. Approximate timings described are based on experience of undertaking landslide assessment after the 2015 Gorkha earthquakes, and related studies, but will inevitably vary between events.

Output	Timescale	Benefits for landslide assessment	Limitations for landslide assessment
Epicenter location, depth, and local magnitude	Seconds - minutes	Rapid event location and scale (magnitude). Earthquake magnitude and depth broadly relates to the scale of landslide impacts, based on e.g., Keefer (1984).	Single point location, rather than impact footprint. Empirical links between earthquake magnitude and landslide impacts have ~ 2 to 3 orders of magnitude of uncertainty, and so preliminary assessments are reliant upon expert judgement. Earthquakes rarely have local, directly comparable precedents, and the spatial distribution of landslides that they trigger is based upon multiple characteristics of the rupture (e.g., area and depth) as well as the overlying topography. Typically focusses response attention to the epicenter, which may not be the most in need.
Modeled shaking intensity, e.g., USGS Shakemap	< 1 h onwards	Identification of area affected by shaking. Can steer relief focus to wider impacted area rather than just epicenter.	Model does not directly predict landsliding, but assumes some correlation between shaking intensity and landslide occurrence. Model is reliant on availability of instrumental records, and is continually updated and refined as new data becomes available. Final version may not be available until weeks-months after the earthquake.
Aerial reconnaissance (e.g., military, expert)	< 1 h onwards	Initial flights, commonly by military, over the affected area can provide a 'first look' assessment of the nature and scale of landslide impacts. Can put limits on the landsliding extent and intensity along the flight track. Systematic flights may follow, enabling more targeted and extensive coverage (e.g., USGS / GEER response described in Collins and Jibson, 2015), as well as analysis of failure evolution / reactivation if an area is revisited.	The route for flights is weather and resource dependent, and may be directed by only limited data, such as the epicenter location. For large earthquakes, complete systematic reconnaissance of the affected area is challenging, and it is unlikely that protocols for mapping impacts are in place at this time. Landslide assessment is unlikely to be the sole purpose of such initial flights, and so systematic data collection is unlikely. Accuracy in locating impacts not directly beneath the flight path can be limited.

Nat. Hazards Earth Syst. Sci. Discuss., https://doi.org/10.5194/nhess-2017-273
Manuscript under review for journal Nat. Hazards Earth Syst. Sci.
Discussion started: 31 July 2017

Natural Hazards and Earth System Sciences
Discussions

Empirically modeled earthquake-triggered landslide maps	< 24 h onwards	Models capable of predicting spatial probability of landslides, footprint and relative intensity of impacts, size distribution, runout, and impact on buildings and infrastructure. Can feed into 72 h Situation Analysis timeframe, and can direct efforts for more detailed assessment. Modelling is independent of weather that might otherwise restrict aerial reconnaissance. Potential to run models in near realtime with ShakeMap.	Heavily reliant on: (1) quality of modeled shaking intensities and availability of instrumental records; (2) availability of input data (e.g., topography, assets); and (3) assumes model training data is sufficient to predict event specific characteristics in hand. Models do not predict individual landslide locations and only provide relative impacts or probabilities which can be difficult to communicate or interpret.
Social media and crowd-sourced information (e.g., Goodchild and Glennon 2010; Barrington et al. 2011; Roche et al. 2013; Poiani et al. 2016).	1 h onwards	Inevitable focus on immediate impacts on population and infrastructure, which is largely unaffected by weather. Can be very agile, with increasing coverage even in remote areas.	Quality control is challenging to enforce as reports are subjective, and locations can be difficult to ascertain. Reliant on functioning communications. Potential bias towards populations / infrastructure restricts ascertainment of total spatial extent and relative intensity of damage, and does not consider more remote latent hazards such as landslide dams. Qualitative local assessments are difficult to extrapolate to relative measures of impact. Critically, no report does not mean no impact.
Polygon of landslide impacts from satellite imagery and estimates of relative intensity of landslide affected areas	First available imagery* + 6 h	Direct positive identification of spatial extent of landslide impacts from optical satellite data captured after the earthquake, where mapping individual landslides is not required to delimit the extent of impacts. Valuable for informing response logistics, and imagery itself provides understandable map of impacts. Can be achieved with medium-resolution imagery (e.g., Landsat). Identification of intense impacts informs location of initial relief delivery and airborne assessments. Can be assessed qualitatively without the need for a full inventory.	Reliant on cloud-free imagery. Lighting, vegetation cover, and steep topography may make interpretation challenging. Landsliding may have poor radiometric contrast with unbroken ground, making landsliding difficult to identify. Subjective definition of severity remains.
Landslide mapping Automatic landslide mapping (e.g.; Martha et al., 2010; Mondini et al., 2011; Lu et al., 2011; Đurić et al., 2017; Hölbling et al., 2017)	First available imagery* + 1 h**	Potentially rapid generation of full landslide inventory across the entire affected area. Time to complete is expected to reduce as technology improves and more experience is gained (Voigt et al., 2016).	Technique still in infancy, restricted to cloud free optical imagery, and reliant upon a style of landsliding that is readily visible in post-earthquake imagery. Use of SAR for rapid inventory generation, in particular through cloud cover, is still in its infancy (e.g., Casagli et al., 2016).
↑	↑	↑	**Products can inform the 72 h Situation Analysis** ↑ ↑ ↑

Nat. Hazards Earth Syst. Sci. Discuss., https://doi.org/10.5194/nhess-2017-273
Manuscript under review for journal Nat. Hazards Earth Syst. Sci.
Discussion started: 31 July 2017

Natural Hazards and Earth System Sciences Discussions

Site-specific landslide dam assessment (e.g., Kargel et al., 2016)	First available imagery* + ~ 3 days onwards	Requires assessment of possible dam locations in the fluvial network across the impacted area and inspection in imagery of known newly formed dams, but critical to complete as quickly as possible after earthquake to mitigate downstream secondary impacts. Not reliant on having full landslide inventory.	Dependent on high resolution cloud free imagery. Ideally benefits from time-series imagery to assess dam evolution and stability, without combining upstream and downstream flow monitoring. Future landslide dam stability remains difficult to forecast.			
Landslide mapping: Full inventory (points) (e.g., Kargel et al., 2016)	First available imagery* + ~ 5 days	Relatively quick to create a full inventory. Enables locations with intense damage to be identified (and hence e.g., roads liable to blockage), and relative intensity of impacts across the affected area to be quantified to guide response resources, and area of landslide impacts to be positively identified. Minimal sensitivity to orthorectification errors in steep topography.	Cloud cover and image acquisition dependent. Limited ability to appraise landslide size, mechanism and risk. Proximity to and impact of landslide on infrastructure difficult to appraise. Landslide numbers alone of questionable value to responders. Hard to manage consistency, and commonly has to be mapped from multiple images from multiple sources, making mapping potentially inconsistent.			
Landslide mapping: Full inventory (polylines) (e.g., This study)	First full available imagery* + ~ 7 days	Relatively quick to create compared to polygons, and requires only slightly more effort relative to points. Polyline length can act as proxy for landslide size, and enables appraisal of landslide proximity to population and infrastructure, providing a binary assessment of location of impacts. Mechanism can be inferred from polyline length (e.g., debris flow v slump).	As above, but estimates of landslide size are potentially susceptible to image distortion particularly in steep topography and off-nadir satellite view directions. Sensitive to instances in which cloud cover partially obscured the landslide track.			
Landslide mapping: Full inventory (polygons) (e.g., Martha et al., 2016; Roback et al., 2017)	First full available imagery* + 2 weeks minimum	Area and volume estimation for scientific use. Allow analysis of future change to landslides (e.g., post-monsoon). Enables full appraisal of landslide proximity to population and infrastructure, and assessment of potential magnitude of impacts.	As above. Arguably limited added benefit for relief effort as compared to polyline mapping. Relatively slow to generate. Highly sensitive to orthorectification and georeferencing errors.			
↑	↑	↑	**Products can inform the two-week MIRA report**	↑	↑	↑

*Refers to the latency of cloud-free image acquisition (typically ~ 24 – 72 h), the duration of which is likely to vary considerably in mountainous regions.

** Estimated duration of automated landslide mapping currently unknown

Nat. Hazards Earth Syst. Sci. Discuss., https://doi.org/10.5194/nhess-2017-273
Manuscript under review for journal Nat. Hazards Earth Syst. Sci.
Discussion started: 31 July 2017

Natural Hazards and Earth System Sciences
Discussions

Figures

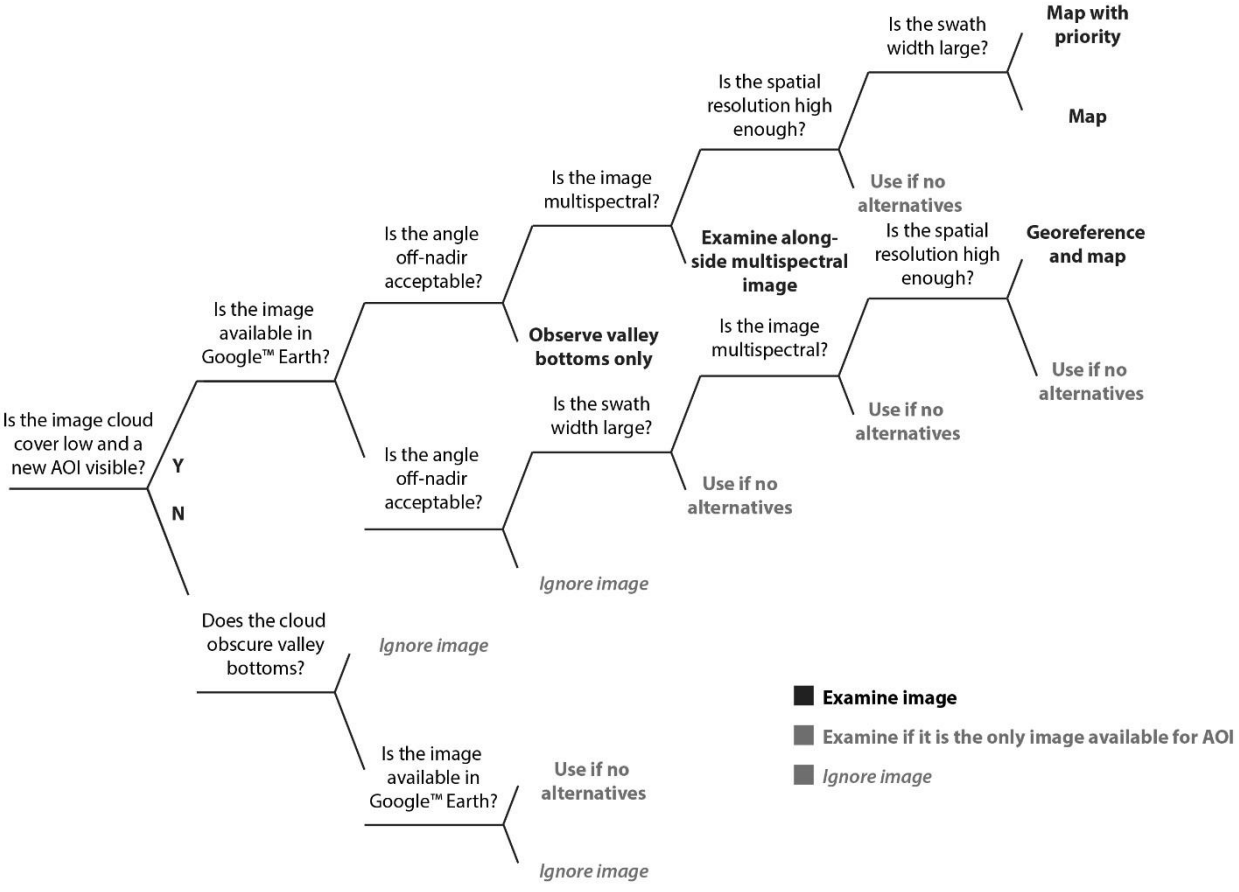

Figure 1. Decision tree for prioritising imagery used for landslide mapping after the 2015 Gorkha earthquake. The relative importance of criteria decreases from left to right. Datasets were prioritised if they were efficient to pre-process and provided high resolution data are optimal for mapping. Imagery with large swath widths and acceptable off-nadir angles may be difficult to acquire in mountainous terrain. These criteria were therefore prioritised to reduce the time spent georeferencing and the number of images required. Given the sub-metre resolution of VHR imagery and the ability to pan-sharpen multispectral imagery, most image resolutions are now sufficient to map landslides with the potential to cause significant damage. Spectral resolution was therefore considered as a more useful criterion for distinguishing landslides of this type than spatial resolution. This decision tree may also be applied to image selection for automated landslide mapping.

Nat. Hazards Earth Syst. Sci. Discuss., https://doi.org/10.5194/nhess-2017-273
Manuscript under review for journal Nat. Hazards Earth Syst. Sci.
Discussion started: 31 July 2017

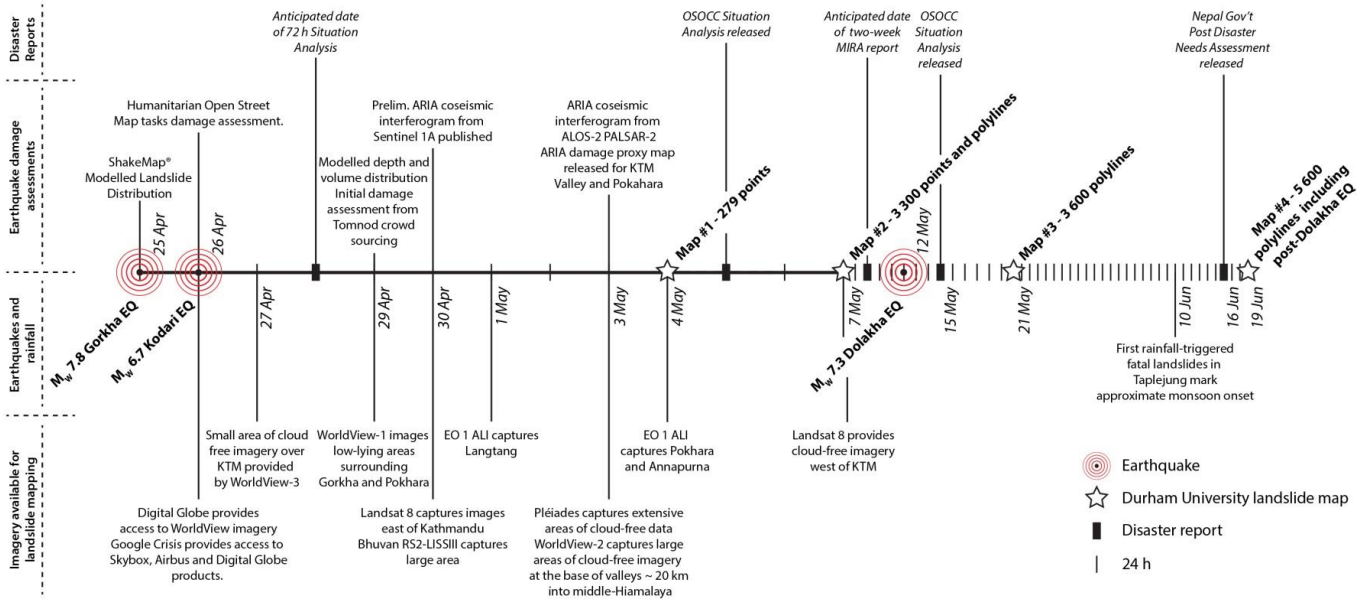

Figure 2: Timeline of image acquisition, mapping, disaster reports, and other earthquake damage assessments from 25 April 2015. Earthquake timing is also added alongside the approximate onset of the monsoon on 10 June (46 days after the Gorkha earthquake). The timing of OCHA On-site Operations Coordination Centre (OSOCC) Situation Analysis reports and the Nepal Government's Post Disaster Needs Assessment (PDNA) are added alongside the proposed timings of the Situation Analysis and MIRA report as defined by IASC (2015). No MIRA report was created following the Nepal earthquakes due to logistical difficulties in organising its creation and physical access constraints (ECHO, 2015). The timeline is not linear, with each vertical line representing one day.

Nat. Hazards Earth Syst. Sci. Discuss., https://doi.org/10.5194/nhess-2017-273
Manuscript under review for journal Nat. Hazards Earth Syst. Sci.
Discussion started: 31 July 2017

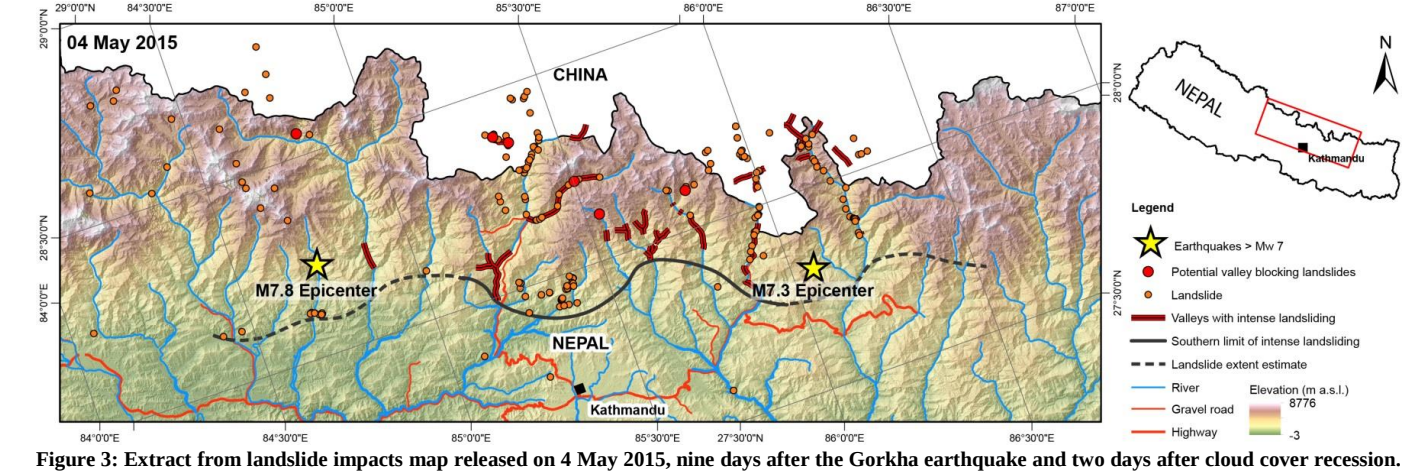

Figure 3: Extract from landslide impacts map released on 4 May 2015, nine days after the Gorkha earthquake and two days after cloud cover recession. Orange dots represent the location of observed individual landslides, at the point at which they reached the valley base. Red dots represent potential valley blocking landslides that had the potential to inhibit river flow, posing a future breach risk downstream. Red lines represent valleys identified as having experienced very intense landsliding, predominantly rockfall and dry debris flows. The black line delimited the southern limit of the area of intense landsliding. This limit was observed where solid and was anticipated where dashed, given that it was not visible in imagery. Both the 25 April (Gorkha) and 12 May (Dolakha) epicenters are added to this map for reference, despite its release prior to the Dolakha earthquake.

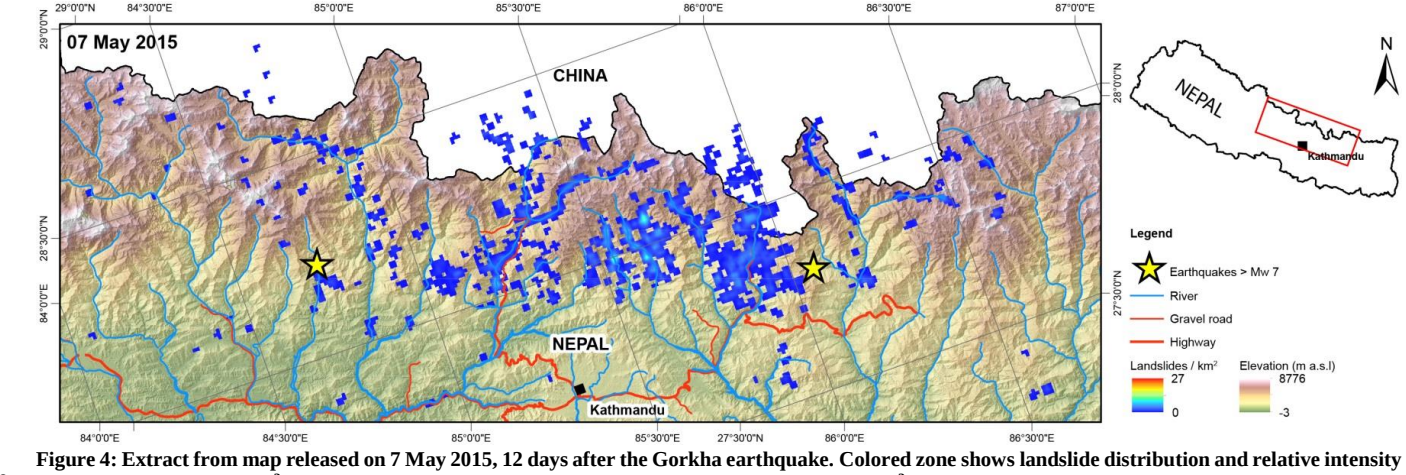

Figure 4: Extract from map released on 7 May 2015, 12 days after the Gorkha earthquake. Colored zone shows landslide distribution and relative intensity (number of landslides / km^2). The colour map has been adjusted to a range of 0-27 landslides / km^2 for comparison between Fig. 4-5. At this point, all areas in the map extent had been assessed using at least pan-sharpened Landsat 8 imagery (15 m). VHR (< 3 m) optical imagery had been used where available.

Nat. Hazards Earth Syst. Sci. Discuss., https://doi.org/10.5194/nhess-2017-273
Manuscript under review for journal Nat. Hazards Earth Syst. Sci.
Discussion started: 31 July 2017

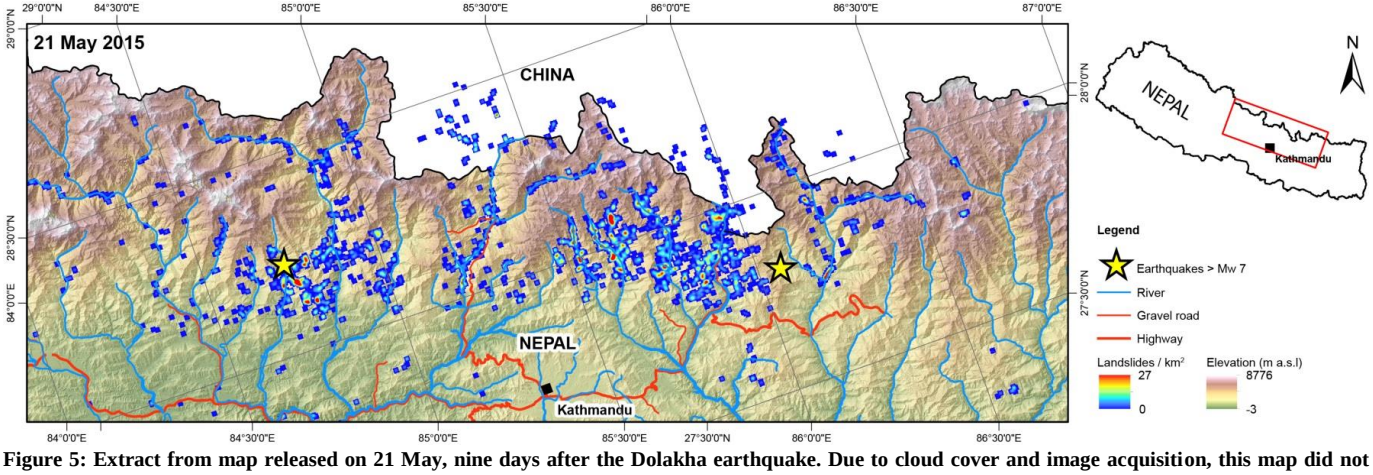

Figure 5: Extract from map released on 21 May, nine days after the Dolakha earthquake. Due to cloud cover and image acquisition, this map did not include landslides that occurred following the Dolakha earthquake.

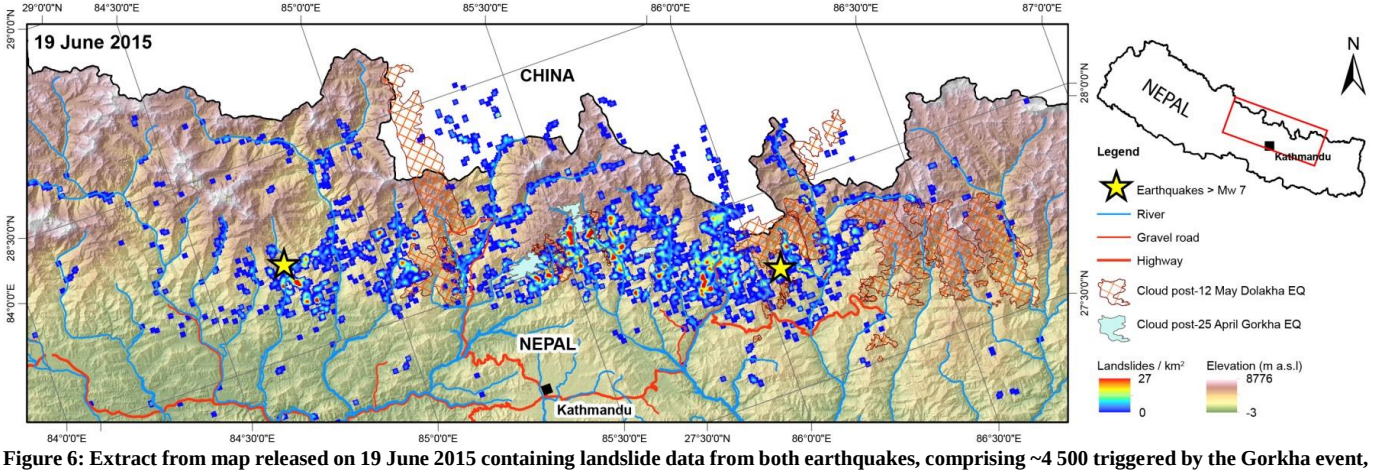

Figure 6: Extract from map released on 19 June 2015 containing landslide data from both earthquakes, comprising ~4 500 triggered by the Gorkha event, ~300 by the Dolakha event, and ~800 that could be attributed to either. Orange hatched pattern highlights areas that could not be mapped following the Dolakha earthquake event. Turquoise pattern (direct north of Kathmandu) highlight areas that remained unmapped following both earthquakes.

Acknowledgements

The research was funded by NERC Urgency Grant NE/N007689/1, the NERC-ESRC 'Earthquakes without Frontiers project (NE/J01995X/1), GCRF Grant NE/P016014/1, and the UK Department for International Development (DfID) as part of the Science for Humanitarian Emergencies and Resilience (SHEAR) program. This study has also been in part supported by the DIFeREns2 (2014-2019) COFUND scheme supported by the European Union's Seventh Framework Programme (#609412). We are grateful to H. Bell and S. Whadcoat from Durham University who provided assistance during the mapping. We thank the various agencies that made satellite imagery freely available through the International Disaster Charter, and in particular C. Jordan and T. Dijkstra from the British Geological Survey. We also thank the United Nations Office for Coordination of Humanitarian Affairs (UN-OCHA) and the UN Resident Coordinator's Office in Kathmandu, and DfID offices in London and Nepal, whose input in helping to define the timelines of useful information for emergency response greatly informed this study.